SAND2000-2950J

Charge-Separation Effects in 1.3μm GaAsSb Type II Quantum Well Laser Gain

W. W. Chow and H. C. Schneider

Sandia National Laboratories, Albuquerque, NM 87185-0601, USA

(October 20, 2000)

Abstract

A microscopic laser theory is used to investigate gain and threshold properties in a GaAsSb quantum well laser. Depending on the geometry of the type-II quantum well gain region, there may be appreciable band distortions due to electron-hole charge separation. The charge separation and accompanying band distortions lead to interesting optical behaviors, such as excitation dependent oscillator strength and bandedge energies. Implications to laser operation include significant blue shift of the gain peak with increasing injection current, and inhibition of spontaneous emission, which may result in threshold current reduction.

DISCLAIMER

Semiconductor gain media in the 1.3 to 1.5 μm wavelength range are currently under intense investigation, because of the important role of lasers in optical fiber communications. For vertical-cavity surface-emitting lasers (VCSELs), gain structures that can be epitaxially grown on GaAs substrates are of particular interest. One such system is the type-II GaAsSb/GaInAs/GaAs quantum well structure. [1–3] The defining feature of a type-II quantum well is the spatial separation of electron and hole confinement in the epitaxial growth direction. Because of the charge separation, a type-II quantum well structure can exhibit interesting excitation dependent optical behaviors due to the competing effects of quantum confinement, which separates the electron and hole distributions, and the resulting Coulomb attraction, which induces band distortions that have the opposite effect of increasing their overlap.

This paper describes a theoretical investigation of the interplay of the competing effects, especially their influence on gain spectra and laser threshold behaviors. Figure 1 depicts the type-II quantum well configuration [1] considered in this paper. To compute the bandstructure, we use $\mathbf{k} \cdot \mathbf{p}$ theory and the envelope approximation. [4] Charge separation effects are incorporated by the simultaneous solution of Poisson's equation and the $\mathbf{k} \cdot \mathbf{p}$ Hamiltonian. Input parameters are the bulk material properties. [2,5,6] The results of the bandstructure calculations, specifically the energy dispersions and optical dipole matrix elements, are used in a microscopic laser model to determine the optical response. This model is based on solving the dynamical equation for the microscopic polarization due to electron-hole pairs. [7] The approach takes into account the many-body modifications to the transition frequency (bandgap renormalization) and the Rabi frequency (Coulomb field renormalization). Dephasing and plasma screening due to carrier-carrier correlations are treated using quantum kinetic equations at the level of the second Born approximation in the Markovian limit. Following semiclassical laser theory, [8] the steady state solution for the microscopic polarization is used in Maxwell's equations to give the optical gain. Considering only the linear optical response to an input laser field, the electron and hole populations are assumed to be constant, and are inputs to the gain calculation.

Figure 2 shows the computed room temperature absorption and gain spectra. We use quantum well structures of different GaInAs and GaAsSb layer thicknesses to illustrate the interplay of the type-II quantum confinement and the excitation dependent charge separation effects. For $w_1 = w_2 = 4nm$ (Fig. 2a), the electron and hole spatial separation is sufficiently small to produce an appreciable dipole matrix element, and negligible band distortions. Consequently, the spectral behavior is very similar to that of a type-I system. For example, the invariance of the exciton absorption peak position during the bleaching of the exciton resonance is maintained. As in type-I quantum wells, this is a consequence of the strong cancellation between the weakening of the exciton binding energy and the reduction of the bandgap energy. At high densities, optical gain appears in the spectral vicinity of the exciton resonance.

For $w_1 = w_2 = 6nm$ (Fig. 2b), the separation between electron and hole wavefunctions increases, which leads to a weak dipole matrix element. As a result, the values of absorption and gain are smaller than those found in the previous example. The $n = 1$ and 2 exciton resonances are closer in energy because of a smaller conduction subband energy separation, which is a direct consequence of the reduced coupling between the identical GaInAs wells. The excitation dependence of the spectra indicates that charge-separation effects are becoming increasingly important. They give rise to a slight blue shift in the exciton resonances with increasing carrier density. This is particularly evident for the $n = 2$ resonance. Similar blue shifts have been observed in other type-II quantum wells. [9] The spectral location of the gain is also blue shifted from the first exciton peak. This can be seen by comparing the gain peak position relative to the dotted line.

The type-II signatures are even more prominent for $w_1 = w_2 = 8nm$ (Fig. 2c). Here, we notice a further reduction in the energy difference between the $n = 1$ and $n = 2$ transitions, and a more pronounced charge-separation induced blue shift of the spectra with increasing carrier density. There are also effects of a strong excitation dependence in the dipole matrix element. The dipole matrix element starts out at low density with a very small value, which is the reason for the low absorption coefficient at the exciton resonance. It then increases

with carrier density because of the charge-separation induced band distortions. At carrier densities where gain is present, the band distortions are sufficiently strong to give a dipole matrix element that is comparable to that of the $w_1 = w_2 = 4nm$ structure. An indication of a strongly excitation dependent dipole matrix element occurs at high photon energies. In Fig. 2c, the spectra show increasing absorption with increasing carrier density. In contrast, Figs. 2a and 2b show an excitation independent absorption at high photon energies.

Figure 3 illustrates the carrier density dependence of peak gain. We find two distinct physical mechanisms for gain in a type-II quantum well. For $w_1 = w_2 = 4nm$, the appearance of gain is due to band filling, as in a type-I quantum well. In contrast, a population inversion already exists in the $w_1 = w_2 = 6nm$ and $8nm$ structures before appreciable gain is present. Here, the onset of gain is due to the restoration of the dipole matrix element by band distortions. Because strong band distortions are necessary for gain to occur in these wider structures, significantly higher carrier densities are necessary. This fact, however, does not mean that wider structures are less suitable as laser gain media.

To compare the merits of the different geometries as gain media, one has to also consider the spontaneous emission loss. We express this loss in terms of a spontaneous emission current density, $J_{sp} = eN_{qw}(w_1 + 2w_2)\int_0^\infty d\omega\ S(\omega)$, where e is the electron charge, N_{qw} is the number of quantum wells in the gain region, and $S(\omega)$ is the spontaneous emission spectrum. To determine $S(\omega)$, we use an expression relating spontaneous emission and gain, that is based on detailed balance. [10] Figure 3b describes the relationship between J_{sp} and the round trip gain, $2\Gamma G_{pk}N_{qw}(w_1 + 2w_2)$, where Γ is the mode confinement factor. We assume a VCSEL with three quantum wells ($N_{qw} = 3$) located at the optical mode antinode ($\Gamma = 2$). The curves give the theoretical limit to the threshold current density for a given round trip gain. They show significantly less sensitivity to quantum well geometry than those in Fig. 3a. This is because changes in the dipole matrix element affects both the gain and spontaneous emission. For comparison, we also plotted the curve for a 5nm $Ga_{0.47}In_{0.53}As/InP$ quantum well (dot-dashed curve), which is representative of a more-developed material system for long-wavelength semiconductor lasers. The higher current

density needed to achieve the same round trip gain in GaInAs/InP can be traced to the higher spontaneous emission loss in this type-I quantum well structure. From the threshold condition we obtain $2\Gamma G_{pk} N_{qw}(w_1 + 2w_2) = 2\alpha_{eff} L_c + \ln(R_1 R_2)$, where $\alpha_{eff} L_c$ represents the single-pass optical losses in the cavity, R_1 and R_2 are the distributive Bragg reflector (DBR) reflectivities, and we assume VCSEL operation at the gain peak. For a typical VCSEL, where absorption in the DBRs is a major contribution to the optical losses, the right hand side gives a round trip loss (or gain) of $\approx 10^{-2}$. According to Fig. 3b, the threshold current densities is around $200 A/cm^2$ for the ideal device (see dotted lines). This is considerably less than measured in experiments. [3,11,12] However, the experimental devices may not have the InGaAs layers for electron confinement, round trip loss are likely to be different, and there is probably significant contribution from non radiative losses, which is neglected in Fig. 3b. An estimation of the non radiative losses in a device may be obtained by comparison of experimental and theoretical transparency current densities. For example, a transparency current density of 134A/cm^2 was reported in Ref. [12]. Based on our calculated transparency current and carrier density of 17A/cm^2/quantum well and 10^{12}cm^{-2}, respectively, we estimated an effective non radiative decay rate of $3 \times 10^9 s^{-1}$ for the experimental device.

Experiments have reported significant shifts of the photoluminescence peak towards higher energy with increasing excitation. [2,11,12] Any blue shift is a concern when the goal is to achieve long wavelength operation. Like the experiments, our calculated spontaneous emission spectra also show sizeable peak shifts. For the three structures considered in this paper, these shifts are relatively linear with carrier density, and they range from 10 to 13meV for a 10^{12}cm^{-2} change in carrier density. Similar shifts are also predicted for the gain spectra. Figure 4 plots the wavelength of the gain peak as a function of round trip gain. For both spontaneous and gain spectra, the blue shift is the net result of the effects of charge separation and band filling (both giving blue shifts), together with band distortions and many-body Coulomb effects (both giving red shifts). Comparison with the GaInAs/InP structure (dot-dot-dashed curve) shows that a large contribution comes from charge sepa-

ration effects. One consequence of the blue shift is a large energy difference between the luminescence peak at low excitation and the lasing emission. Assuming a VCSEL with a round trip gain of 10^{-2}, we found for this difference, 20, 24 and 27 meV for the 40, 60 and 80nm layer thickness structures. These values are consistent with experiment. [12] Even higher energy differences are possible for lasers operating with high threshold gains. For example, at high carrier densities, where the first excited conduction subband contribution to the gain is appreciable, energy differences between the low excitation luminescence peak and the lasing emission can be over 100meV.

In summary, the microscopic calculations of optical gain in type-II GaInSbAs/GaInAs/GaAs quantum well structures predict interesting geometry and excitation dependences in optical properties, because of the interplay of type-II quantum confinement and charge separation. These two competing effects can lead to oscillator strength and bandedge energies that vary with carrier density. As a result, there may be a significant blue shift of the gain peak with increasing injection current, and inhibition of spontaneous emission in a laser device.

This work was supported in part by the U. S. Department of Energy under contract No. DE-AC04-94AL85000. We thank O. Blum and J. F. Klem for helpful discussions.

REFERENCES

[1] J. R. Meyer, C. A. Hoffman and F. J. Bartoli, Appl. Phys. Lett. **67**, 757 (1995).

[2] M. Peter, K. Winkler, M. Maier, N. Herres, J. Wagner, D. Fekete, K. H. Bachem and D. Richards, Appl. Phys. Lett. **67**, 2639 (1995).

[3] T. Anan, M. Yamada, K. Tokutome, S. Sugou, K. Nishi and A. Kamei, Electron. Lett. **35**, 903 (1999).

[4] G. Bastard, *Wave Mechanics Applied to Semiconductor Heterostructures*, (Les Editions de Physique, Paris 1988).

[5] *Landolt-Börnstein*, edited by O. Madelung (Springer, Berlin, 1987), Vol. 22a.

[6] W. Braun, P. Dowd, C.-Z. Guo, S. L. Chen, C. M. Ryu, U. Koelle, S. R. Johnson, Y.-H. Zhang, J. W. Tomm, T. Elsässer and D. J. Smith, J. Appl. Phys. **88**, 3004 (2000).

[7] W. W. Chow and S. W. Koch, *Semiconductor-Laser Fundamentals: Physics of the Gain Materials* (Springer, Berlin, 1999).

[8] W. E. Lamb, Jr., Phys. Rev. **134**, A1429 (1964).

[9] G. R. Olbright, W. S. Fu, A. Owyoung, J. F. Klem, R. Binder, I. Galbraith and S. W. Koch, Phys. Rev. Lett. 66, 1358 (1991).

[10] C. H. Henry, R. A. Logan and F. R. Merritt, J. Appl. Phys. **51**, 3042 (1980).

[11] T. Anan, K. Nishi, S. Sugou, M. Yamada, K. Tokutome and A. Gomyo, Electron. Lett. **34**, 2127 (1998).

[12] O. Blum and J. F. Klem, IEEE Photonics Tech. Lett. **12**, 771 (2000).

Figure Captions

Figure 1. Electron and hole confinement energies in a type-II GaInSbAs/GaInAs/GaAs quantum well structure.

Figure 2. Calculated TE absorption/gain spectra for $GaAs_{0.7}Sb_{0.3}/Ga_{0.85}In_{0.15}As/GaAs$ type-II structure at $T = 300K$. The layer thicknesses are $w_1 = w_2 =$ (a) $4nm$, (b) $6nm$, and (c) $8nm$. The carrier densities are $N = 0.2$ to $1.8 \times 10^{12} cm^{-2}$ in $2 \times 10^{11}\ cm^{-2}$ increments.

Figure 3. (a) Peak gain vs. carrier density and (b) round trip gain vs. spontaneous emission current density for $GaAs_{0.7}Sb_{0.3}/Ga_{0.85}In_{0.15}As/GaAs$ type-II structures, at $T = 300K$ and with $w_1 = w_2 = 4nm$ (solid curve), $6nm$ (dashed curve), and $8nm$ (dot-dashed curve). The dot-dot-dashed curve is for a 5nm $In_{.53}Ga_{.47}As/InP$ type-I quantum well structure.

Figure 4. Gain peak wavelength vs. round trip gain. All parameters and notations are similar to those in Fig. 3.

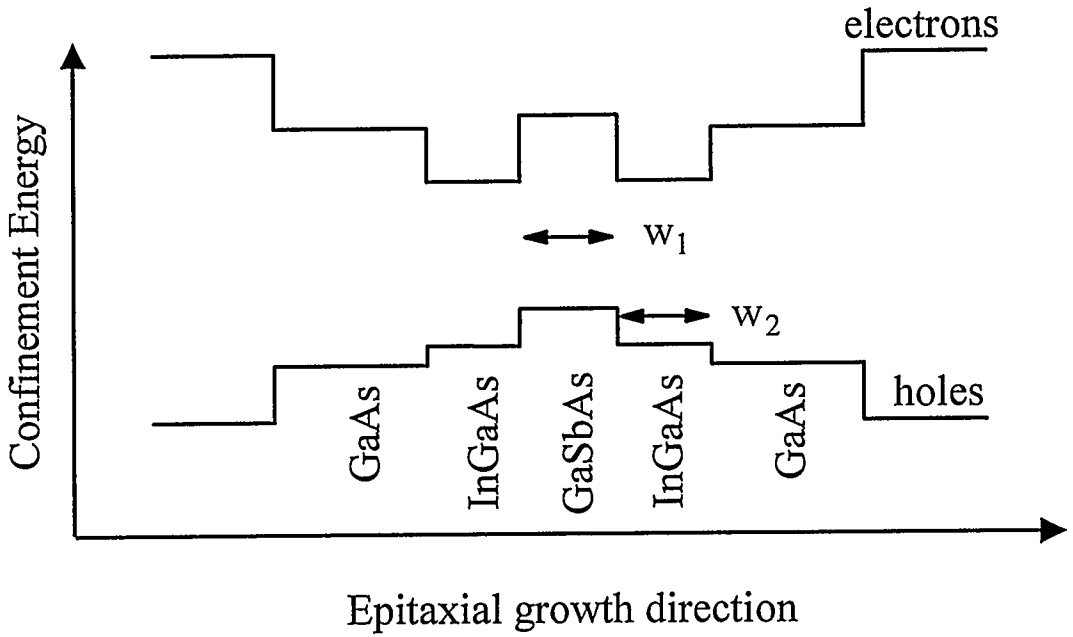

Fig. 1, APL, Chow

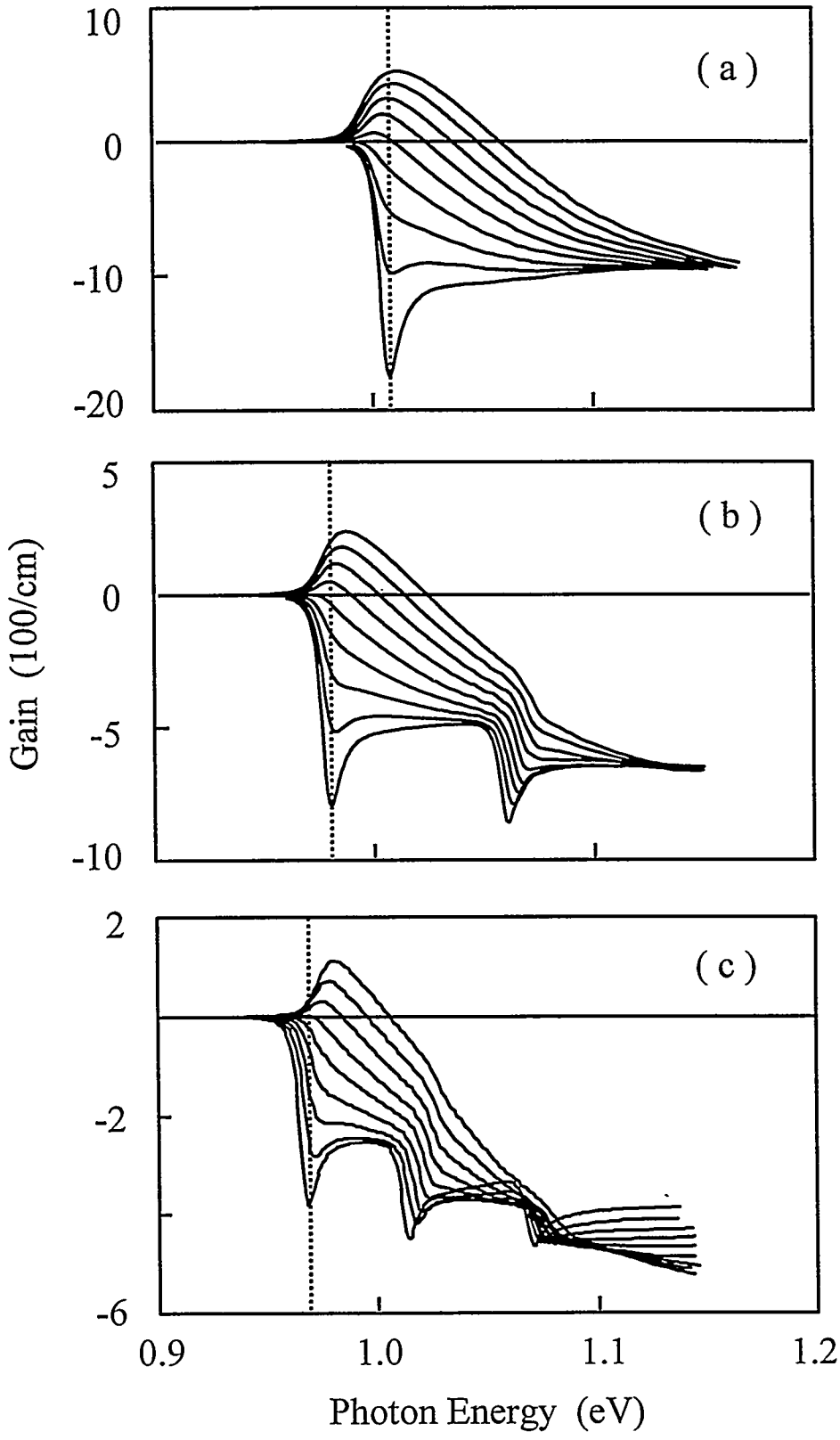

Fig. 2, APL, Chow

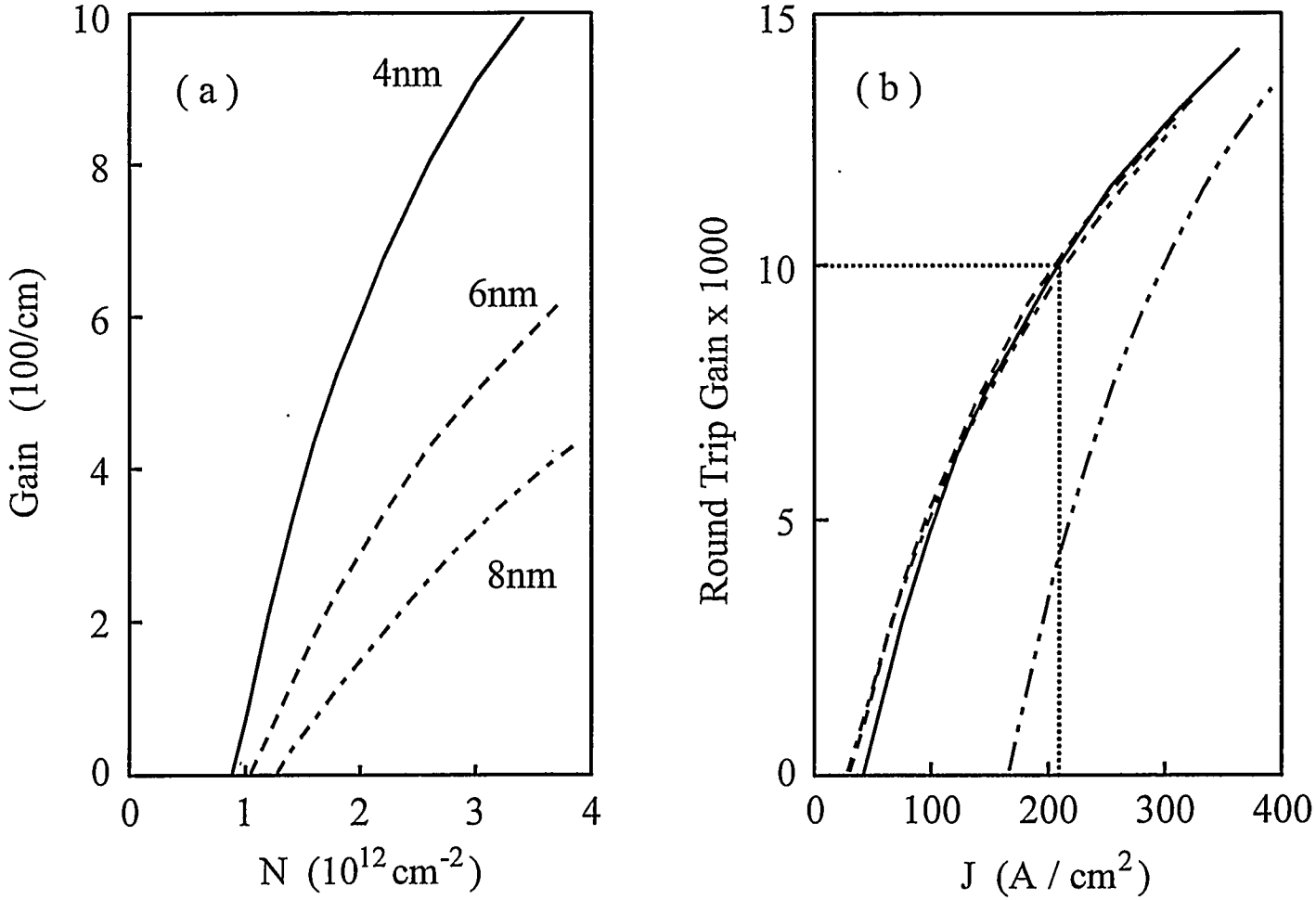

Fig. 3, APL, Chow

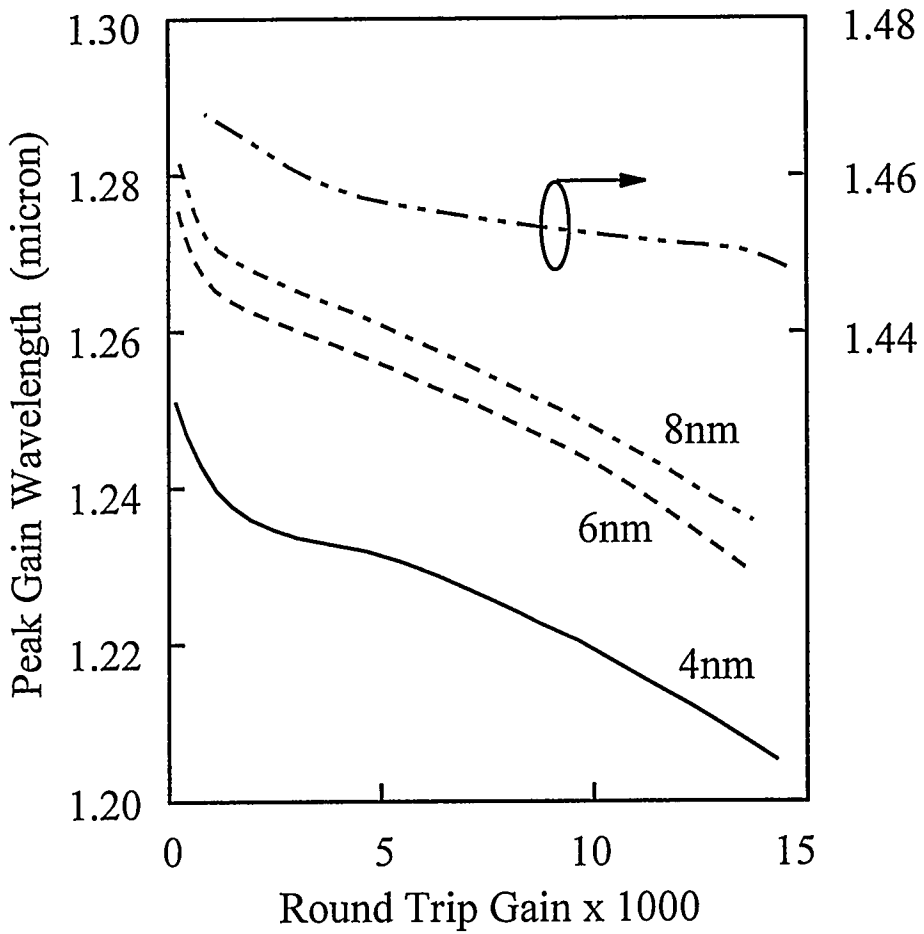

Fig. 4, APL, Chow